Bull. Mater. Sci., Vol. 37, No. 3, May 2014, pp. 721–728. © Indian Academy of Sciences.

Pulse electrodeposition and corrosion properties of Ni–Si_3N_4 nanocomposite coatings

S KASTURIBAI[1,2] and G PARUTHIMAL KALAIGNAN[2,*]

[1]Department of Chemistry, Alagappa Government Arts College, Karaikudi 630 003, India
[2]Advanced Nanocomposite Coatings Laboratory, Department of Industrial Chemistry, Alagappa University, Karaikudi 630 003, India

MS received 28 January 2013; revised 20 April 2013

Abstract. **The development of modern technology requires metallic materials with better surface properties. In the present investigation; Si_3N_4-reinforced nickel nanocomposite coatings were deposited on a mild steel substrate using pulse current electrodeposition process employing a nickel acetate bath. Surface morphology, composition, microstructure and crystal orientation of Ni and Ni–Si_3N_4 nanocomposite coatings were investigated by scanning electron microscope, energy dispersive X-ray spectroscopy and X-ray diffraction analysis, respectively. The effect of incorporation of Si_3N_4 particles in the Ni nanocomposite coating on the micro hardness, corrosion behaviour has been evaluated. Smooth composite deposits containing well-distributed silicon nitride particles were obtained and the crystal grains on the surface of Ni–Si_3N_4 composite coating are compact. The crystallite structure was face centred cubic (*fcc*) for electrodeposited nickel and Ni–Si_3N_4 nanocomposite coatings. The micro hardness of the composite coatings (720 HV) was higher than that of pure nickel (310 HV) due to dispersion-strengthening and matrix grain refining and increased with the increase of incorporated Si_3N_4 particle content. The corrosion potential (E_{corr}) in the case of Ni–Si_3N_4 nanocomposite had shown a negative shift, confirming the cathodic protective nature of the coating.**

Keywords. **Pulse electro deposition; nanocomposite coating; XRD; SEM; microhardness.**

1. Introduction

Electrodeposition by pulse electrolysis has received much attention in recent years. The development of modern technology requires metallic materials with better surface properties. The need for composites with improved resistance to highly aggressive environments is high as a result of a growing demand for extended safe service life of industrial objects. Composite plating produced by co-deposition of powders with a metal has been widely applied to the aerospace, automotive, manufacturing, chemical processing and hydraulics industries. Particle-reinforced metal matrix composites generally exhibited wide engineering applications due to their enhanced hardness, better wear and corrosion resistance, when compared to pure metal or alloy (Jeon *et al* 2008). Nanocomposites of a metallic matrix containing dispersion of second phase particles usually display a variety of novel properties. Electro-co-deposition is a low-cost and low-temperature suitable process to fabricate nanocomposite coatings. Numerous nanostructured metals, alloys and metal matrix composites have been successfully produced by electrodeposition (Kim and Oh 2011).

The structure and properties of composite coatings depend not only on the concentration, size, distribution and nature of the reinforced particles, but also the electroplating parameters such as current density, temperature, pH value, etc. Among these factors, the type of applied current is one of the most important parameters (Li *et al* 2009). It is well known that the pulsed-electrodeposition technique has been used successfully to produce bulk nanostructure metals, alloys and nanocomposite coatings with high purity, low porosity and unique material properties (Karathanasis *et al* 2010). The pulsed-electrodeposition process distinguishes itself from the conventional direct current processes mainly in the high peak current density and the on-time and off-time alternatives. The use of pulse-electrodeposition technique permits electrolysis with a very high current density for a short period of time, i.e., a very high deposition rate is achieved during the on-time. The relaxation period in pulse plating enables higher current to be applied during the transient period without reactant concentration depletion. Adjustment of the deposition parameter can change the grain size, twin density and crystallographic texture so that one is able to contrive mechanical properties (Lajevardi and Shahrabi 2010). The structure of electroplated metal and alloy coatings is specified by the electrocrystallization process, particularly by the interplay

*Author for correspondence (pkalaignan@yahoo.com)

between nucleation and crystal growth (Alfantazi *et al* 1996). An attractive way of controlling these two processes is the application of a periodically changing current (Shen *et al* 2008). Compared to direct current plating, pulse plating can yield nanocrystalline coatings with improved surface appearance and properties, such as smoothness, refined grains and enhanced corrosion resistance (Ranjith and Paruthimal Kalaignan 2010). Moreover, nanocrystalline coatings with improved surface appearance and mechanical properties can be obtained by pulse electroplating (Borkar and Harimkar 2011). The properties of metals, alloys and composite coatings can be controlled and enhanced by modifying their microstructure, when using pulse current (Wang *et al* 2010). A number of oxides, carbides and nitrides were used as second phase particles to produce composite coatings. Silicon nitride (Si_3N_4) is a very hard ceramic material and possesses excellent dimensional stability. Hence, Si_3N_4 has also been used to reinforce metallic coatings and it improves hardness, wear resistance and corrosion resistance (Rajiv *et al* 1995; Li *et al* 2011). Si_3N_4 co-deposition was carried out with Ni, Co and Fe as the metallic components (Shi *et al* 2005; Khazrayie and Aghdam 2010). There is no literature available for Ni– Si_3N_4 nanocomposite coatings in acetate-based bath. Acetate-based baths are environmental friendly compared to other baths (Ranjith *et al* 2011).

In this present work, a pure nickel and nanocrystalline metallic composite coatings were prepared by the pulsed electrodeposition in a nickel acetate bath and the bath containing Si_3N_4 particles, respectively. The microstructure and surface morphology of the nanocomposite coatings were investigated by X-ray analysis, scanning electron microscope (SEM) and energy dispersive X-ray spectroscopy (EDX) analysis, respectively. The micro hardness was measured by Vickers micro-hardness tester. The corrosion resistance of the nanocomposite coatings were evaluated by electrochemical impedance and Tafel polarization studies. The microstructure and properties of the Ni–Si_3N_4 nanocomposite coatings are also compared with the pure Ni coatings deposited under similar pulsed-electrodepositing conditions.

2. Experimental

2.1 *Materials, chemicals and instruments used*

Mild steel specimens were used as a base material for the deposition of Ni composites. The mild steel specimens were given the following sequential pre-treatment before the electrodeposition. (i) Degreasing with trichloroethylene, (ii) alkaline electro cleaning, (iii) washed with running water, (iv) mild acid dip in 5% (v/v) hydrochloric acid for 10 s, (v) washed with running water and (vi) distilled water dip. All the chemicals used for carrying out the experiments were of AR grade. Triple-distilled water was used for the preparation of bath solutions. Myriad bipolar-pulsed power supply was used as pulse current power source for all deposition studies.

2.2 *Bath preparations and plating conditions*

For any electroplating, proper method of preparing baths and pre-conditioning the solutions to remove metallic and other impurities is an essential part to get good deposits of required physical and chemical properties. The plating bath electrolyte composition and electroplating parameters are given in table 1. The pure nickel and Ni–Si_3N_4 nanocomposite plating was carried out in a 500 mL glass beaker containing nickel acetate bath and with suspended Si_3N_4 particles, respectively. Nickel bar of high purity (99·9%) was used as the anode and pre-treated MS plate specimen ($4 \times 2{\cdot}5$ cm) was used as cathode. By means of magnetic stirrer, the suspended particles were thoroughly stirred and a fine uniform suspension was thus obtained in the bath. The effect of plating was monitored with the various concentrations of Si_3N_4 particles in suspension at constant current density (8 A dm^{-2}). The boric acid and sodiumdodecylsulphate were used as buffer and wetting agent, respectively.

2.3 *Hardness, structural and morphological analysis*

Vickers hardness was measured at an applied load of 50 g for 15 s. The hardness measured for a set of three points across the diameter of the disks from which a mean value and standard deviation were calculated. The structural analysis of the coatings were performed by using X-ray diffraction (XRD) method by using an X'Pert PRO diffractometer with CuKα radiation ($\lambda = 0{\cdot}15406$ nm). The crystallite size was calculated for both pure Ni and Ni–Si_3N_4 nanocomposite coatings by using the following Scherrer's equation (Krawitz 2001).

$$\text{FWHM} = \frac{K\lambda}{D\cos\theta}\frac{180^\circ}{\pi}, \tag{1}$$

where FWHM is the full width half maxima in 2θ degrees, D the crystallite size in nanometres, K constant (usually evaluated as 0·94) and the wavelength of CuKα radiation is 0·154 nm. For surface analysis, HITACHI S-570, scanning electron microscope was used. The weight percentage of each element in the coating was determined by energy dispersive X-ray analysis (EDX) coupled with SEM on different locations at the surface.

2.4 *Corrosion measurements*

Potentiodynamic polarization and impedence measurements were conducted using an electrochemical analyser

Table 1. Optimized bath composition and pulse electroplating conditions.

Electrolyte composition and pulse parameters	
Nickel acetate – 150 g L^{-1}	Current density – 8 Ad m^{-2}
Nickel chloride – 55 g L^{-1}	pH – 4·5
Boric acid – 35 g L^{-1}	Temperature – 30 °C
Sodiumdodecylsulphate – 0·05 g L^{-1}	Plating time – 45 min
Silicon nitride (1 μm) – 3–15 g L^{-1}	Stirring speed – 150 rpm
Frequency – 10 Hz	Duty cycle – 50%

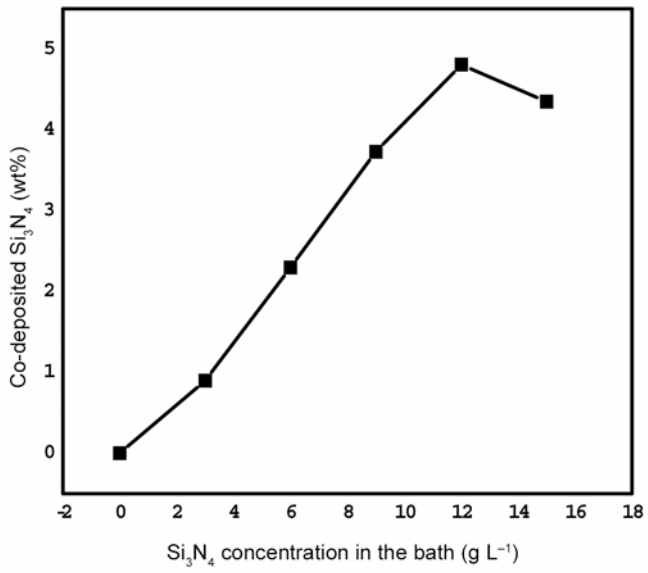

Figure 1. Effect of amount of Si_3N_4 in bath (in grams per litre) on weight percentage of Si_3N_4 in nanocomposite coatings.

(EG&G – Auto Lab Analyzer Model: 6310) connected to a PC for potential control and data acquisition. Corrosion experiments were carried out in 3·5 wt% NaCl solution at room temperature. The coated mild steel specimen was masked with lacquer to expose 1 cm^2 area which served as the working electrode. Pt foil (1 cm^2) was used as the counter electrode and a saturated calomel electrode (SCE) act as the reference. The potentiodynamic polarization studies were carried out for the potential range from –0·75 to –1·25 V with respect to the OCP at a scan rate of 2 mV/s. The potential E (V vs SCE) was plotted against log I (A cm^{-2}) to obtain polarization curve. From this polarization curves, the corrosion potential (E_{corr}) and corrosion current (i_{corr}) of the specimens were obtained using the Tafel extrapolation method. Impedance measurements were performed at the open circuit potential of –0·71 mV after the immersion of sample for 1 min in 3·5 wt% NaCl solution. The same three electrode cell setup was used for this experiment. The impedance spectra were recorded in the frequency range of 10 kHz–100 mHz.

3. Results and discussion

3.1 *Effect of particle concentration on co-deposition*

The variation of loading in bath solution and the amount of its inclusion in the deposit are shown in figure 1. It is evident that the increase in the bath loading from 3 to 12 g L^{-1} Si_3N_4 at the fixed current density of 8 A dm^{-2} at 30 °C, the amount of particles co-deposited were also increased. The maximum amount of Si_3N_4 inclusion was noticed at 12 g L^{-1} of Si_3N_4 in the bath solution, which is in agreement with the earlier observation (Xue *et al* 2006). The increase in the co-deposited nanoparticulates with increasing Si_3N_4 particulates content in the electrolyte can be explained by Guglielmi's (1972) two-step adsorption model. In other words, a higher concentration of Si_3N_4 particulates in the electrolyte enhanced the adsorption rate, thus resulting in a higher weight percentage of the co-deposited Si_3N_4 nano-particulates. But beyond 12 g L^{-1} of Si_3N_4, the weight percentage of the co-deposited Si_3N_4 particulates decreases, may be due to agglomeration of nano-sized particles in the plating bath.

3.2 *Effect of current density*

The effect of current density on the content of the co-deposited Si_3N_4 from a bath containing 12 g L^{-1} of Si_3N_4 particle at 30 °C is shown in figure 2. It is observed that the content of the co-deposited Si_3N_4 nanoparticulates increases initially with the current density and reaches a maximum at 8 A dm^{-2}. Beyond this current density, the weight percentage of the co-deposited Si_3N_4 particulates decreases. Before the maximum 8 A dm^{-2}, the increasing content of Si_3N_4 can be attributed to the increasing tendency for adsorbed particles to arrive in the cathode surface, which is in consistent with Guglielmi's (1972) model. The process is controlled by the adsorption of the particles and the particle deposition is dominant. At higher current densities, there will be an increase in the hydrogen evolution and a decrease in the Ni electrodeposition efficiency. As a result of this, $Ni(OH)_2$ will be formed near the cathode, which favours the co-deposition process. This result is in agreement with earlier observations (Shi *et al* 2006). When current density is greater than 8 A cm^{-2}, the decreasing trend can be explained by

the fact that an increase in current density results in more rapid deposition of the metal matrix and fewer particles are embedded in the coating, since the latter is dependent mainly on the hydrodynamic conditions in the electrolyzer.

3.3 *X-ray diffraction analysis*

The crystallite size and phase structure of the electrodeposited nickel and Ni–Si_3N_4 nanocomposite coatings were calculated by using XRD analysis (figure 3). Its corresponding XRD data is given in table 2. First, the crystallite sizes of pure Ni coatings as well as Ni–Si_3N_4 nanocomposite coatings were calculated by using FWHM of prominent (111) reflection in the Scherrer's equation. The calculated crystallite size for pure Ni coating was ~ 21 nm, which is significantly greater than that for Ni–Si_3N_4 nanocomposite coating of ~ 19 nm. This indicates that the reinforcement of Si_3N_4 in nickel resulted in refinement of the microstructure of the composite coatings. The crystallite structure was *fcc* for electrodeposited nickel and Ni–Si_3N_4 nanocomposite coatings. It was confirmed from the nickel ICDD–JCPDS standards (70-0989). The preferred growth process of the nickel matrix in crystallographic directions (111), (200) and (220) is strongly influenced by Si_3N_4 nanoparticles. The peak width of the Ni–Si_3N_4 nanocomposite coating is slightly broader than that of Ni coating. This is attributed to the reduction in the grain size of the nanocomposite coating by the addition of Si_3N_4 particles. This indicates that the Si_3N_4 particles get adsorbed on the growing crystal and inhibit its further growth resulting in small-sized crystals. This makes the crystals more compact and indirectly assists in generating more nucleation sites for the reduction of Ni^{2+} ions from bath solution.

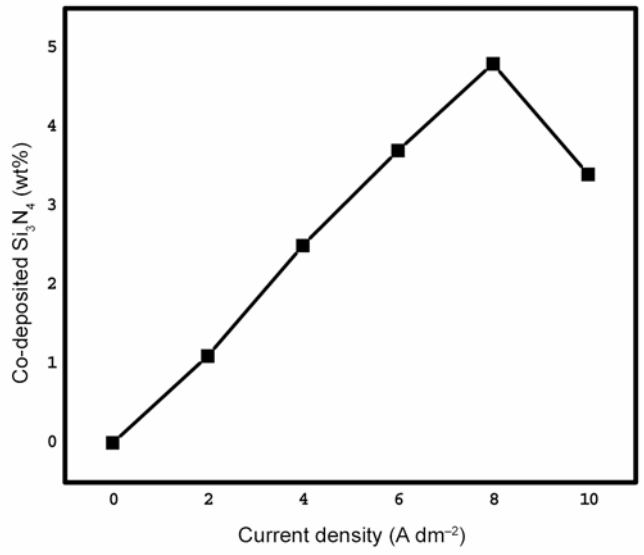

Figure 2. Effect of current density on weight percentage of Si_3N_4 in nanocomposite coatings containing Si_3N_4 (12 g L^{-1}).

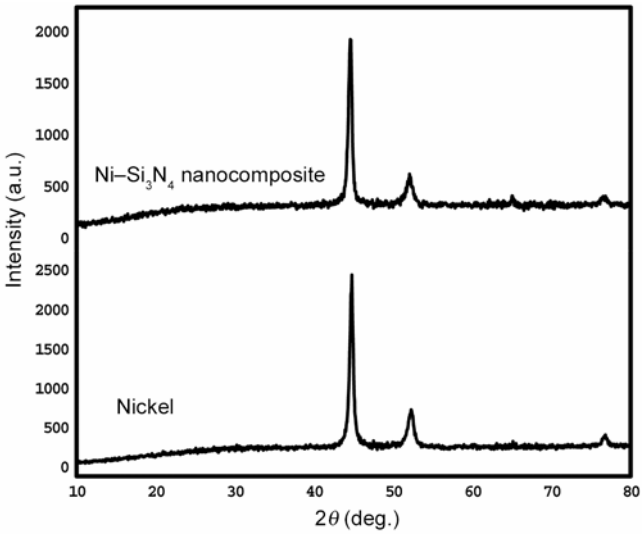

Figure 3. XRD patterns of (**a**) electrodeposited nickel and (**b**) Ni–Si_3N_4 nanocomposite coating.

3.4 *EDX spectra analysis*

The EDX spectra of the Ni–Si_3N_4 (4·9 wt%) nanocomposite coating obtained by the addition of 12 g L^{-1} Si_3N_4 is shown in figure 4. The EDX spectrum shows that Si peak indicating the presence Si_3N_4 in the Ni matrix. This confirms that, the substrate is covered with Ni–Si_3N_4 nanocomposite coating, which is in good agreement with previous considerations. The EDX analysis of Ni–Si_3N_4 nanocomposite coating gives the average elemental percentages of Si, N and Ni as 2·1, 2·6 and 95·3, respectively.

3.5 *SEM analysis*

The SEM morphologies of the electrodeposited nickel and Ni–Si_3N_4 nanocomposite coating were shown in figures 5(a and b). Smooth and well-crystallized nanocomposite deposits with good distribution of Si_3N_4 particles were obtained. Ni–Si_3N_4 nanocomposite coating is characterized by particulate-like structure, which indicates that the co-deposited Si_3N_4 nanoparticulates are much uniformly distributed in the Ni matrix of the nanocomposite coating. In addition, many nodular agglomerated grains are seen on the nanocomposite coating surface (figure 5b). It is supposed that the co-deposited Si_3N_4 nano-particulates of a fairly uniform distribution and agglomeration to some extent may contribute to increasing the hardness and corrosion resistant properties of the nanocomposite coatings. It shows that Ni–Si_3N_4 nanocomposite coating is fairly uniform, continuous and compact.

Table 2. XRD parameters of pulse electrodeposited nickel and Ni–Si_3N_4 nanocomposite coatings.

Electro-deposits	*d*-spacing (Å)		Miller indices	Lattice parameter (*a*)		Str./phase	Average crystallite size (nm)
	Observed	Standard		Observed	Standard		
Nickel	2·02602	2·0297	111	3·512	3·515	*fcc*	21
	1·75175	1·7578	200				
	1·24205	1·2429	220				
Ni–Si_3N_4 (12 g L^{-1}) composite	2·02527	–	111	3·510	3·515	*fcc*	19
	1·75260	–	200				
	1·24400	–	220				

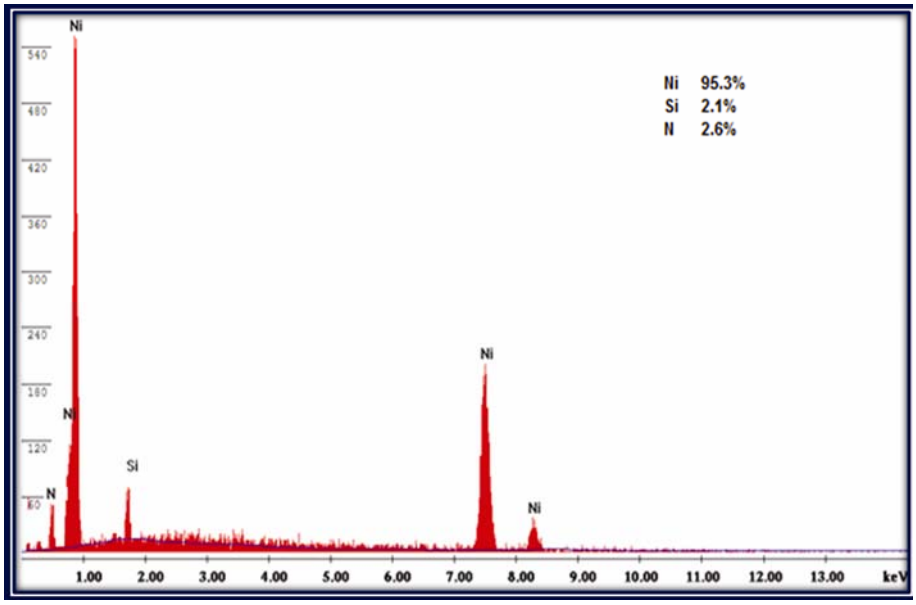

Figure 4. EDAX analysis spectrum of electrodeposited Ni–Si_3N_4 (12 g L^{-1}) nanocomposite coatings.

3.6 *Effect of particle loading on micro hardness*

Vickers micro hardness measurements were performed for pulse electrodeposited nickel and Ni–Si_3N_4 nanocomposite coatings are shown in figure 6. The Ni–Si_3N_4 nanocomposite coatings exhibited significantly improved micro hardness (720 HV) compared to pure nickel coatings (310 HV). The micro hardness of the nanocomposite coatings were increased with Si_3N_4 particles content in the nickel matrix. Similar to that, has been reported in Ni–CeO_2 (Xue *et al* 2006). The embedding of nanoparticles as the second phase, perturbs the crystal growth of Ni, inducing a reduction in the crystal size, gives deposits with significantly increased hardness values. The intensification in the hardness of Ni–Si_3N_4 nanocomposite coating was due to grain refining and dispersive strengthening effect caused by the dispersion of Si_3N_4 nanoparticles in the nanocomposite coatings. The grain-fining and dispersive strengthening effects have become stronger with increasing nano–Si_3N_4 content. Thus, the micro hardness of the Ni–Si_3N_4 composite coatings was increased with increasing Si_3N_4 content. The thickness of pure nickel and composite coatings were 17 μm and around 20 μm, respectively (Kasturibai and Paruthimal Kalaignan 2013).

3.7 *Electrochemical impedance measurements*

Electrochemical impedance measurements for the electrodeposited nickel and Ni–Si_3N_4 nanocomposite coatings are shown in figure 7(a). The obtained Nyquist curves consist of one capacitive loop. The more pronounced frequency arcs were obtained for the sample coated with nanocomposite layer. The equivalent circuit $R_S - R_{ct}$/CPE which was used to fit the parameters is shown in figure 7(b) and the derived parameters are given in table 3, where CPE is a constant phase element, *n* is the phase shift which can be explained as a degree of surface inhomogeneity (Solmaz *et al* 2011). Generally, the use of CPE is required due to the distribution of relaxation times as a result of inhomogenities present at a micro level or

nano level such as the surface roughness and porosity. The charge transfer resistance (R_{ct}) values for Ni–Si_3N_4 nanocomposite coatings were increased and the constant phase element (CPE) values decreased with increased Si_3N_4 content in the nanocomposite coatings. This behaviour is usually assigned to changes in density and composition of electrode coating. It is revealed that nanocomposite coatings were more corrosion resistance than the electrodeposited nickel coatings.

3.8 *Tafel measurements*

The Tafel curves were measured for the electrodeposited nickel and Ni–Si_3N_4 nanocomposite coating in 3·5 wt% NaCl (figure 8). The corrosion current (I_{corr}), corrosion potential (E_{corr}), corrosion rates (CR), Tafel slopes b_a and b_c were obtained from the Tafel plots (table 4). Corrosion rates (CR) were calculated by the following equation (Vathsala and Venkatesha 2011).

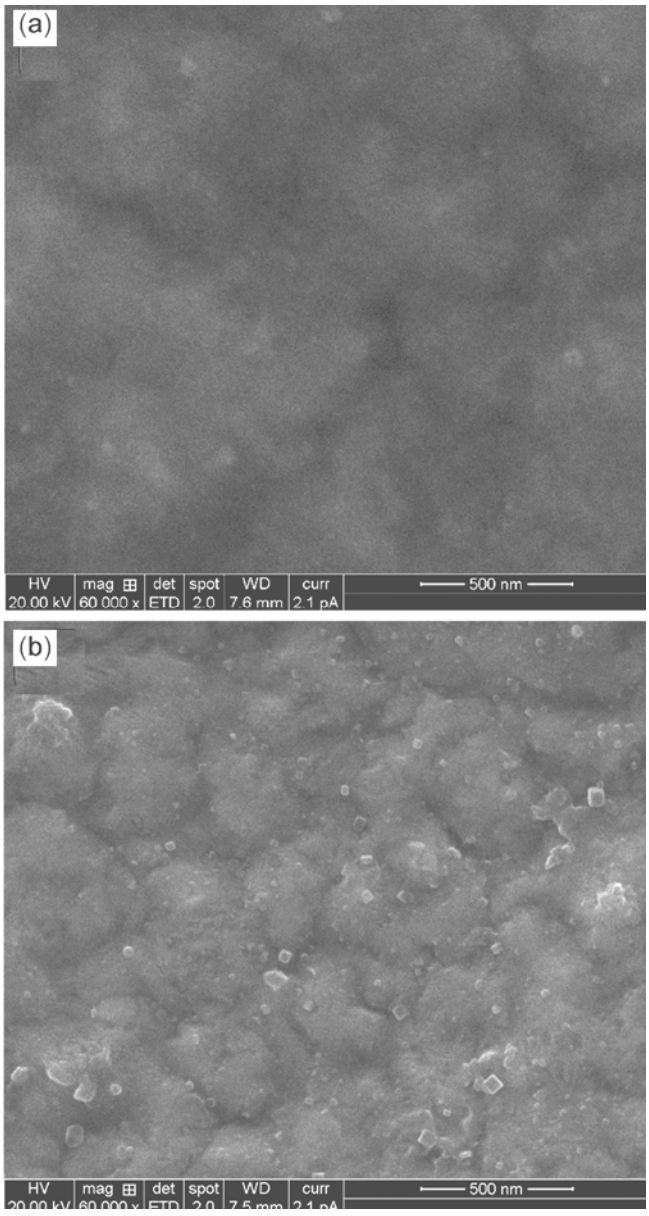

Figure 5. SEM photographs of (**a**) electrodeposited nickel and (**b**) Ni–Si_3N_4 (12 g L^{-1}) nanocomposite coatings.

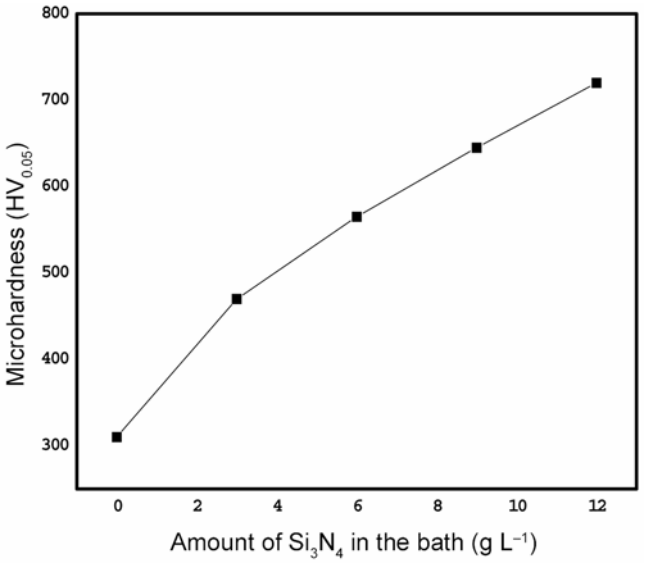

Figure 6. Effect of Si_3N_4 content on hardness of coatings.

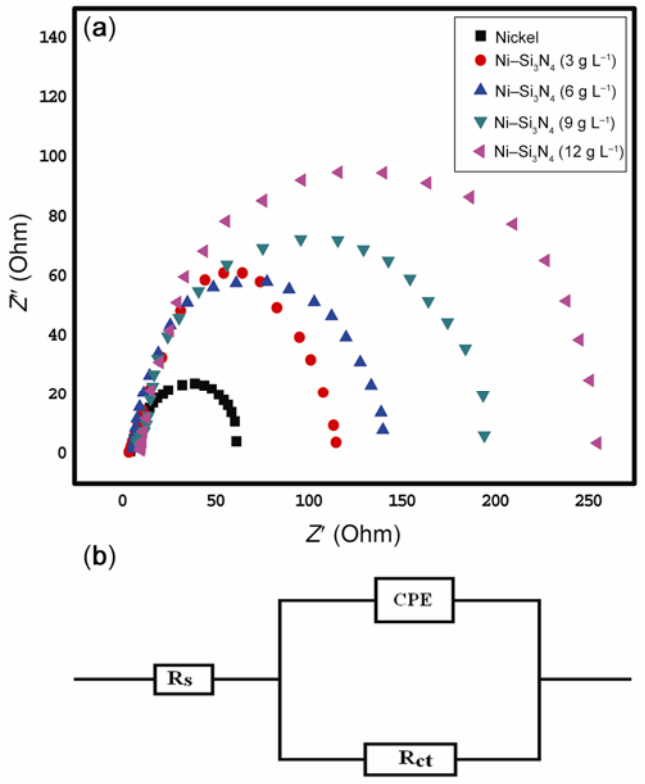

Figure 7. (**a**) Nyquist diagrams of impedance spectrum of electrodeposited nickel and Ni–Si_3N_4 nanocompositie coatings. (■) Electrodeposited nickel, (●) Ni–Si_3N_4 (3 g L^{-1}), (▲) Ni–Si_3N_4 (6 g L^{-1}), (▼) Ni–Si_3N_4 (9 g L^{-1}) and (◀) Ni–Si_3N_4 (12 g L^{-1}) and (**b**) equivalent electrical circuit.

Table 3. Parameters derived from impedance measurements of pulse electrodeposited nickel and Ni–Si_3N_4 nanocomposite coatings.

Material	R_s (Ω cm^{-2})	R_{ct} (Ω cm^{-2})	n	CPE (F cm^{-2}) $\times 10^{-6}$
Nickel	5·457	55·72	0·8177	150·90
Ni–Si_3N_4 (3 g L^{-1})	6·022	110·65	0·8542	105·70
Ni–Si_3N_4 (6 g L^{-1})	6·449	132·81	0·8906	83·50
Ni–Si_3N_4 (9 g L^{-1})	9·916	188·44	1·0236	35·60
Ni–Si_3N_4 (1 2g L^{-1})	10·34	241·54	1·2363	14·89

Table 4. Tafel polarization parameters of pulse electrodeposited nickel and Ni–Si_3N_4 nanocomposite coatings.

			Tafel slope		
Material	E_{corr} (V vs SCE)	I_{corr} (μA/cm^2)	β_a	β_c	CR (milliinch/yr)
Nickel	–0·633	81·22	107	102	69·69
Ni–Si_3N_4 (3 g L^{-1})	–0·716	67·09	82	76	56·11
Ni–Si_3N_4 (6 g L^{-1})	–0·863	05·01	62	58	4·33
Ni–Si_3N_4 (9 g L^{-1})	–0·882	03·16	66	54	2·73
Ni–Si_3N_4 (12 g L^{-1})	–0·906	01·25	64	58	1·08

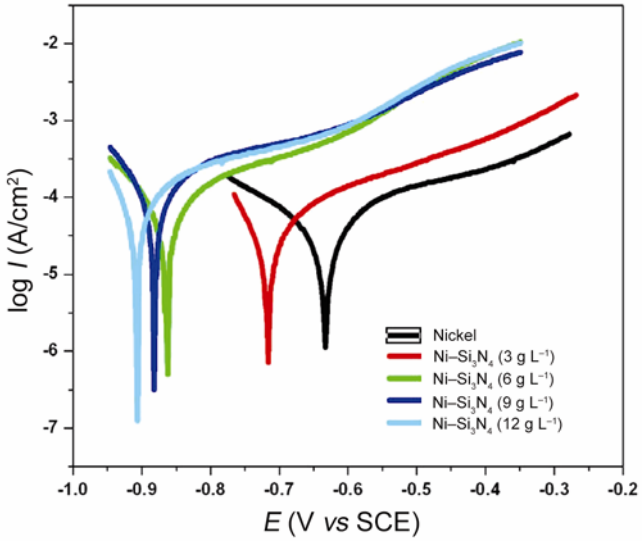

Figure 8. Potentiodynamic polarization curves of electrodeposited nickel and Ni–SiO_2 nanocompositie coatings. (**a**) Electrodeposited nickel, (**b**) Ni–Si_3N_4 (3 g L^{-1}), (**c**) Ni–Si_3N_4 (6 g L^{-1}), (**d**) Ni–Si_3N_4 (9 g L^{-1}) and (**e**) Ni–Si_3N_4 (12 g L^{-1}).

$$\text{CR (milliinch/yr)} = \frac{kI_{corr}(\text{eq. wt.})}{d}, \quad (2)$$

where $K = 0{\cdot}13$ milliinch g/μA cm yr, I_{corr} is in μA cm^{-2}, eq. wt. is the equivalent weight and d is the density of the nickel metal in g/cm^3. It is seen that the nanocomposite coating has less negative corrosion potentials and smaller corrosion current densities than the Ni coatings. It indicates that the nanocomposite possess better corrosion resistance compared to pure nickel coating. The values of the anodic and cathodic Tafel coefficients for nanocomposite coatings were different from that of pure nickel coating. The change of values was due to the modifications induced on the deposit's surface by the particle co-deposition. This suggested that the presence of Si_3N_4 nanoparticles in nickel coating influences the kinetics of both the anodic and cathodic electrochemical reactions. The corrosion potential (E_{corr}) in the case of Ni–Si_3N_4 nanocomposite coatings had shown a negative shift, confirming the cathodic protective nature of the coating (Ramalingam *et al* 2009). The shift to a lower value in the reduction potential is attributed to a decrease in the active surface area of the cathode, owing to the adsorption of the Si_3N_4 particulates, and may also relate to the decrease in the ionic transport by the Si_3N_4 nanoparticulates. Ni–Si_3N_4 nanocomposite coatings (CR = 1·08 milliinch/yr) were more corrosion resistant than the pulse electrodeposited nickel coating (CR = 69·69 milliinch/yr) in 3·5% NaCl solution. That is the Ni–Si_3N_4 nanocomposite coatings have lower chemical activity than the pure Ni coating and hence, possess better chemical stability in the external environment.

4. Conclusions

Pure nickel and Ni–Si_3N_4 nanocomposite coatings were successfully fabricated using pulse electrodeposition process employing an acetate bath. The reinforcement of Si_3N_4 in the composite coating has prohibited the columnar growth of the nickel grains resulting in random texture and smaller coating thickness in the nanocomposite coatings. The Si_3N_4 reinforcement has further refined the crystallite size in the nanocomposite coatings. The Ni–Si_3N_4 nanocomposite coatings have exhibited significantly improved micro hardness (720 HV) compared to pure nickel coatings (310 HV), due to a combination of

dispersion-strengthening and matrix grain refining. The Ni–Si_3N_4 nanocomposite coatings were more corrosion resistant than the pulse electrodeposited nickel coating in 3·5% NaCl solution. The better corrosion resistance of the Ni–Si_3N_4 nanocomposite coatings may be ascribed to the favourable chemical stability of the Si_3N_4 nanoparticulates, which help to reduce the hole size in the nanocomposite coatings and prevent the corrosive pits from growing up.

Acknowledgement

The authors thank The Head, Department of Physics, Alagappa University, Karaikudi for providing the XRD analysis to carry out this research work.

References

Alfantazi A M, Page J and Erb U 1996 *J. Appl. Electrochem.* **26** 1225

Borkar T and Harimkar S 2011 *Surf. Eng.* **27** 524

Guglielmi N 1972 *Electrochem. Soc.* **119** 1009

Jeon Y S, Byun J Y and Oh T S 2008 *J. Phys. Chem. Solids* **69** 880

Karathanasis A Z, Pavlatou E A and Spyrellis N 2010 *J. Alloys Compd.* **494** 396

Kasturibai S and Paruthimal Kalaignan G 2013 *Ionics* **19** 5

Khazrayie M A and Aghdam A R S 2010 *Trans. Nonferrous Met. Soc. China* **20** 1017

Kim S K and Oh T S 2011 *Trans. Nonferrous Met. Soc. China* **21** 68

Krawitz A 2001 *Introduction to diffraction in materials science and engineering* (New York: John Wiley & Sons, Inc.) p. 165

Lajevardi S A and Shahrabi T 2010 *Appl. Surf. Sci.* **256** 6775

Li J M, Yin J Y, Cai C, Zhang Z, Li J F, Yang J F, Xue M Z and Liu Y G 2012 *Mater. Corr.* **63** 620

Li Q, Yang X, Zhanga L, Wanga J and Chena B 2009 *J. Alloys Comp.* **482** 339

Rajiv E P, Iyer A and Seshadri S K 1995 *Bull. Electrochem.* **11/7** 317

Ramalingam S, Muralidharan V S and Subramania A 2009 *J. Solid State Electrochem.* **13** 1777

Ranjith B and Paruthimal Kalaignan G 2010 *Appl. Surf. Sci.* **25** 42

Ranjith B and Paruthimal Kalaignan G 2011 *Ionics* **17** 495

Shen Y F, Xue W Y, Wang Y D, Liu Z Y and Zuo L 2008 *Surf. Coat. Technol.* **202** 5140

Shi L, Sun C, Gaoa P, Zhou F and Liu W 2006 *Appl. Surf. Sci.* **252** 3591

Shi L, Sun C F, Zhou F and Liu W M 2005 *Mater. Sci. Eng.* **A397** 190

Solmaz R, Altunbas E and Kardas G 2011 *Mater. Chem. Phys.* **125** 796

Vathsala K and Venkatesha T V 2011 *Appl. Surf. Sci.* **257** 8929

Wang J L, Xu R D and Zhang Y Z 2010 *Trans. Nonferrous Met. Soc. China* **20** 839

Xue Y J, Jia X Z, Zhou Y W, Ma W and Li J S 2006 *Surf. Coat. Technol.* **200** 5677